Journal of Hazardous Materials 163 (2009) 835–842

Contents lists available at ScienceDirect

Journal of Hazardous Materials

journal homepage: www.elsevier.com/locate/jhazmat

# Synthesis and characterization of $CuO/Ce_{1-x}Ti_xO_2$ catalysts used for low-temperature CO oxidation

Zhi-Qiang Zou, Ming Meng*, Li-Hong Guo, Yu-Qing Zha

*Tianjin Key Laboratory of Applied Catalysis Science & Engineering, Department of Catalysis Science & Technology, School of Chemical Engineering & Technology, Tianjin University, Tianjin 300072, PR China*

ARTICLE INFO

*Article history:*
Received 20 April 2008
Received in revised form 21 June 2008
Accepted 5 July 2008
Available online 16 July 2008

*Keywords:*
Surfactant
$CuO/CeO_2$
Ti doping
CO oxidation

ABSTRACT

A series of $CuO/Ce_{1-x}Ti_xO_2$ catalysts used for low-temperature CO oxidation were prepared by impregnation with the support derived from surfactant-assisted co-precipitation. The techniques of $N_2$ adsorption/desorption, X-ray diffraction (XRD), X-ray photoelectron spectroscopy (XPS) and temperature-programmed reduction by $H_2$ ($H_2$-TPR) were employed for catalyst characterization. It is found that the support $CeO_2$ prepared by the surfactant-assisted method possesses much larger specific surface area than the one obtained from conventional precipitation. Doping Ti in the support with Ti/Ce atomic ratio of 1:9 or 3:7 can further increase the surface area of $CeO_2$ and decrease its crystallite size. As a result, the active Cu species possess higher dispersion on the support $Ce_{1-x}Ti_xO_2$ than on pure $CeO_2$. The strong interaction between the dispersed Cu species and the support $Ce_{1-x}Ti_xO_2$ makes the catalysts possess much higher oxidation activity and thermal stability. However, when the ratio of Ti/Ce reaches 5:5, opposite effect is found, due to the highest surface concentration of Ti and the lack of surface highly dispersed copper species.



## 1. Introduction

Environment pollution has been a troublesome problem for many years. Carbon monoxide emitted from automobile exhausts and many industrial processes, has become a major air pollutant. Noble metals, such as Pt, have been considered to be effective catalysts for low-temperature CO oxidation [1]; however, the high prices limit their wide use. In the past several years, much attention has been paid to base metals, especially to copper [2–4].

It is known that ceria possesses high oxygen storage capacity provided by the redox couple $Ce^{4+}/Ce^{3+}$ [5]. In $CuO–CeO_2$ binary oxides, a strong catalytic synergy effect between copper oxide and ceria has ever been found [6]. Furthermore, if a third component such as Zr or Sn, was introduced into $CuO–CeO_2$ system, better thermal stability and redox property can be achieved [7–9]. Luo et al. [10] have found that the addition of Ti atoms into $CeO_2$ can significantly improve the storage capacity of mobile oxygen of $CeO_2$ by increasing the reduction extent of the mixed oxides. Zhu et al. [11] studied the supported catalyst of Pd on $CeO_2–TiO_2$ mixed oxide used for CO oxidation and found that the special Pd–Ce–Ti interaction is favorable to the reduction of PdO and interfacial $CeO_2$ species. However, as far as we know, copper supported on Ce–Ti–O mixed oxides used for low-temperature CO oxidation is scarcely reported. The modified storage capacity of $CeO_2$ by $TiO_2$ may also promote the activity of supported Cu species for CO oxidation. Therefore, this work focuses on the copper catalysts supported on a series of $Ce_{1-x}Ti_xO_2$ oxides.

It is well known that a high specific surface area of the support is helpful to disperse the component impregnated on it. In our previous studies [12–14], it is found that when surfactants are involved in the precipitation process, much higher surface areas can be obtained. So a modified co-precipitation method was used for the preparation of Ce–Ti–O mixed oxide, in which the surfactant P123 ($HO(CH_2CH_2O)_{20}(CH_2CH(CH_3)O)_{70}(CH_2CH_2O)_{20}H$) was used as a template. The techniques of nitrogen adsorption/desorption (BET), X-ray diffraction (XRD), X-ray photoelectron spectroscopy (XPS), and the temperature-programmed reduction by $H_2$ ($H_2$-TPR) were used for catalyst characterization. The effect of Ti/Ce ratio on the structures and properties of the supported copper catalysts was discussed in detail.

## 2. Experimental

### 2.1. Catalyst preparation

The mixed oxide supports were prepared by co-precipitation involving the surfactant Pluronic P123 ($HO(CH_2CH_2O)_{20}(CH_2CH(CH_3)O)_{70}(CH_2CH_2O)_{20}H$) participated in the process. Take

* Corresponding author. Tel.: +86 22 2789 2275; fax: +86 22 2789 2275.
*E-mail address:* mengm@tju.edu.cn (M. Meng).

0304-3894/$ – see front matter © 2008 Elsevier B.V. All rights reserved.
doi:10.1016/j.jhazmat.2008.07.035

the sample with Ti/Ce ratio of 5:5 as an example, 0.02 mol of $Ce(NO_3)_3{\cdot}6H_2O$, 0.02 mol of $TiCl_4$ and 0.001 mol of P123 were dissolved in 100 mL distilled $H_2O$, respectively. Then the three kinds of solutions were mixed under stirring, giving a clear homogeneous solution, which was continuously stirred for 2 h. Afterwards, about 15 mL ammonia was quickly added under vigorous stirring to form a solid precipitate. The pH was adjusted to around 9.5. The resulting gel mixture was stirred for 4 h at room temperature and subsequently transferred to Teflon autoclaves, which was kept at 80 °C for 24 h to increase the degree of condensation. The solid product was filtered, washed with water and ethanol, dried in air at 110 °C and finally calcined in air at 500 °C for 4 h. The other supports with different Ti/Ce ratios were prepared in a similar way, keeping the total amount of Ti and Ce unchanged. For comparison, the two kinds of pure $CeO_2$ supports were also prepared by the surfactant-assisted co-precipitation above and the conventional precipitation, which are denoted as $CeO_2$-MP and $CeO_2$-P, respectively. The prepared Ti-containing supports were denoted as $Ce_{1-x}Ti_xO_2$, hereby the $x/(1-x)$ represents the atomic ratio of Ti to Ce. The $CuO/Ce_{1-x}Ti_xO_2$ catalysts were prepared by incipient wetness impregnation, giving Cu content of 6 wt%. The fresh samples were calcined at 500 °C in air for 4 h, while the aged samples were additionally treated at 700 °C in air for 4 h, which are denoted as $CuO/Ce_{1-x}Ti_xO_2$ (A).

### 2.2. Catalyst characterization

The measurement of the specific surface area ($S_{BET}$) and the pore diameter distribution was carried out at 77 K on Quantachrome QuadraSorb SI instrument by using the nitrogen adsorption/desorption method. The samples were pretreated in vacuum at 300 °C for 8 h before experiments. The $S_{BET}$ was determined from the linear part of the BET curve. The pore diameter distribution was calculated from the desorption branch of $N_2$ adsorption/desorption isotherms using the Barrett–Joyner–Halenda (BJH) formula.

XRD patterns were recorded on an X'pert Pro diffractometer (PANAlytical Company) with a rotating anode using Co Kα as radiation source (λ = 0.1790 nm) at 40 kV and 40 mA. The data of $2\theta$ from 10° to 90° range were collected with the step size of 0.02°. Diffraction peaks of crystalline phases were compared with those of standard compounds reported in the JCPDS Data File. The particle sizes were calculated using Scherrer equation.

XPS analysis was performed in a PHI-1600 ESCA SYSTEM spectrometer with Mg Kα as X-ray source (1253.6 eV) under a residual pressure of $5 \times 10^{-6}$ Pa. The error of the binding energy is ±0.2 eV and the C1s ($E_b$ = 284.6 eV) of the contaminated carbon was used as a standard for binding energy calibration.

Temperature-programmed reduction (TPR) measurement was conducted on a TPDRO 1100 apparatus supplied by Thermo-Finnigan Company. Each time, 30 mg of the sample were heated from room temperature to 900 °C at a rate of 10 °C/min. A mixture gas consisting of $H_2$ and $N_2$ with $H_2$ content of 5 vol% was used as reductant at a flow rate of 20 mL/min. Before detection by the TCD, the gas was purified by a trap containing CaO + NaOH materials in order to remove the $H_2O$ and $CO_2$. The operation conditions meet the well-known TPR criteria of Monti and Baiker equation [15].

### 2.3. Catalytic activity test

The catalytic activities of the samples for CO oxidation were measured in a fixed-bed quartz tubular reactor (i.d. 8 mm) mounted in a tube furnace equipped with K-type thermocouples. About 1.0 g catalyst (40–60 mesh) is loaded in the quartz reactor. The temperature of catalyst bed is monitored and controlled by temperature controllers. The reaction mixture containing 1.0 vol% CO, 5.0 vol% $O_2$ and balance $N_2$ is fed to catalyst bed at a space velocity of 30,000 $h^{-1}$. The effluent gas from the reactor was analyzed by a gas chromatograph (BFS, SP 3420) equipped with a thermal conductivity detector and a flame ionization detector.

## 3. Results and discussion

### 3.1. $N_2$ adsorption and desorption (BET)

The $N_2$ adsorption/desorption isotherms and the corresponding pore size distributions of the fresh catalysts, namely CuO supported on $CeO_2$ and $Ce_{1-x}Ti_xO_2$ oxides prepared by using surfactant P123, are shown in Fig. 1. It can be seen that the isotherms are classical type IV, characteristic of mesoporous materials as defined by IUPAC [16]. Well-defined H-2 type hysteresis loops with a sloping adsorption branch and a relatively steep desorption branch are observed at high relative pressure ($P/P_0$) range. This H-2 type hysteresis loop is typical for wormhole-like structures and hierarchical scaffold-like mesoporous structures formed by surfactant-assisted nanoparticle assembly [17]. No regular TEM images were obtained, indicating that the ordered mesoporous structures have not formed in the catalysts. However, the inset figure shows that the fresh samples possess uniform mesopore size distributions.

The texture data of all the fresh samples as well as the aged ones are listed in Table 1. The specific surface areas of the supports calcined at 500 °C are also given in the brackets. By comparing the surface areas of the two kinds of $CeO_2$ prepared by conventional precipitation and surfactant-modified methods, it can be seen that when the surfactant P123 is involved in the preparation process, much larger surface area of $CeO_2$ can be achieved. As illuminated in our previous studies [12–14], during the calcination of the samples, the burn-up of the surfactant will leave pores in the samples, which results in the increase of surface areas, pore volumes and even pore diameters. When different amounts of Ti are doped in the samples, the surface areas are further increased, with the largest one of 161 $m^2/g$ for $Ce_{0.5}Ti_{0.5}O_2$. After Cu was supported on these oxides, a

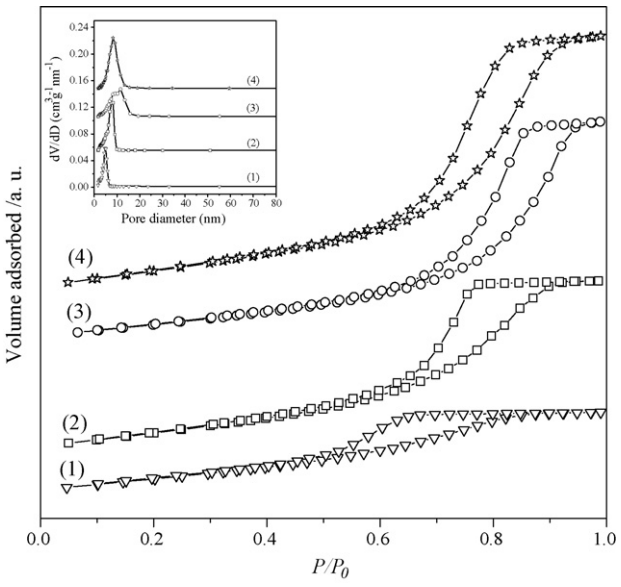


**Fig. 1.** Nitrogen adsorption/desorption isotherms and pore diameter distributions (inset) of the mesoporous samples calcined at 500 °C: (1) $CuO/CeO_2$-MP; (2) $CuO/Ce_{0.9}Ti_{0.1}O_2$; (3) $CuO/Ce_{0.7}Ti_{0.3}O_2$; (4) $CuO/Ce_{0.5}Ti_{0.5}O_2$.

**Table 1**
Physical structure data of the fresh and aged samples

| Sample | $S_{BET}$ ($m^2$/g) | Pore diameter (nm) | Pore volume ($cm^3$/g) | $CeO_2$ crystallite sizes (nm) | $CeO_2$ lattice parameter (Å) |
|---|---|---|---|---|---|
| $CuO/CeO_2$-P | 53 (57)[a] | 3.7 | 0.066 | 12.6 | 5.410 |
| $CuO/CeO_2$-MP | 91 (104)[a] | 4.8 | 0.125 | 7.3 | 5.409 |
| $CuO/Ce_{0.9}Ti_{0.1}O_2$ | 114 (146)[a] | 8.3 | 0.245 | 5.0 | 5.379 |
| $CuO/Ce_{0.7}Ti_{0.3}O_2$ | 102 (122)[a] | 11.6 | 0.299 | 5.3 | 5.376 |
| $CuO/Ce_{0.5}Ti_{0.5}O_2$ | 133 (161)[a] | 8.3 | 0.357 | 9.9 | 5.368 |
| $CuO/CeO_2$-P (A) | 7 | – | 0.014 | 22.3 | 5.415 |
| $CuO/CeO_2$-MP (A) | 32 | – | 0.054 | 17.6 | 5.413 |
| $CuO/Ce_{0.9}Ti_{0.1}O_2$ (A) | 28 | – | 0.122 | 10.3 | 5.379 |
| $CuO/Ce_{0.7}Ti_{0.3}O_2$ (A) | 32 | – | 0.185 | 10.3 | 5.387 |
| $CuO/Ce_{0.5}Ti_{0.5}O_2$ (A) | 15 | – | 0.099 | 12.8 | 5.403 |

[a] The data in brackets are the specific surface areas of the corresponding supports.

little decrease in the surface areas can be observed from Table 1 but the catalyst $CuO/Ce_{0.5}Ti_{0.5}O_2$ still shows the largest surface area and pore volume. When the samples were aged at 700 °C, their surface areas and pore volumes greatly decreased, the $CeO_2$-P supported catalyst shows the lowest surface area of only 7 $m^2$/g, which is less than a half of those for other samples. At the same time, it can be seen that the samples with the atomic ratio of Ti/Ce equal to 1:9 and 3:7 possess higher thermal stability. These results indicate that the atomic ratio of Ti/Ce plays an important role in enlarging the surface areas of the supports and increasing their thermal stability.

### 3.2. Bulk and surface composition

The XRD patterns of the fresh samples $CuO/Ce_{1-x}Ti_xO_2$ are presented in Fig. 2. The peaks around $2\theta = 33.3°$, 55.7°, 66.5°, 38.6°, 69.8° and 82.8° obviously indicate the presence of the fluorite structure typical of $CeO_2$ in all the samples. Besides, two weak featured diffraction peaks of CuO can be found in the pure $CeO_2$ supported samples . For clarity, the enlarged patterns from $2\theta$ of 40–50° are shown as an inset in Fig. 2. However, no peaks attributed to CuO crystal phase could be observed for the samples $CuO/Ce_{1-x}Ti_xO_2$, implying that CuO is more finely dispersed on $Ce_{1-x}Ti_xO_2$ mixed oxides. At the same time, no diffraction peaks ascribed to Ti-containing oxides can be observed, either, suggesting that Ti may be incorporated into the $CeO_2$ lattice while maintaining the fluorite structure.

Fig. 3 shows the XRD patterns of the aged samples. It can be seen that evident CuO peaks at $2\theta = 41.5°$ and 45.3° appear in all the samples resulting from the sintering. By comparing the diffraction peaks assigned to $CeO_2$ and CuO appearing in the XRD patterns for the aged samples without Ti doping, it is found that many other peaks appear in the XRD patterns for the aged samples doped with Ti. However, these diffraction peaks cannot be attributed to any known Ti- or Ce-containing compounds according to the current available ICDD files. Usually, Ce- and Ti-containing oxides easily form some complicated compounds when calcined at high temperatures. Rynkowski et al. [18] have also found some diffraction peaks that cannot be ascribed to any phases for their Ce–Ti mixed oxides calcined at 800 °C. Luo et al. [10] reported a similar phenomenon for the $Ce_xTi_{1-x}O_2$ mixed oxide materials synthesized by a sol–gel method. The very small peak at $2\theta = 29.5°$ present in the XRD pattern for the aged sample $CuO/Ce_{0.7}Ti_{0.3}O_2$ (A) suggests the formation of some anatase phase.

The average crystallite sizes and lattice parameters derived from the crystal plane (1 1 1) of $CeO_2$ in both the fresh and the aged samples are listed in Table 1. For the two samples without Ti doping, it is noted that the $CeO_2$ in the sample prepared by surfactant-modified method shows smaller crystallite size. Doping Ti in the sample has further decreased the size of crystallites $CeO_2$. Meanwhile, the lattice parameters of $CeO_2$ for the fresh samples become much smaller after Ti doping. This means that $Ti^{4+}$ may be

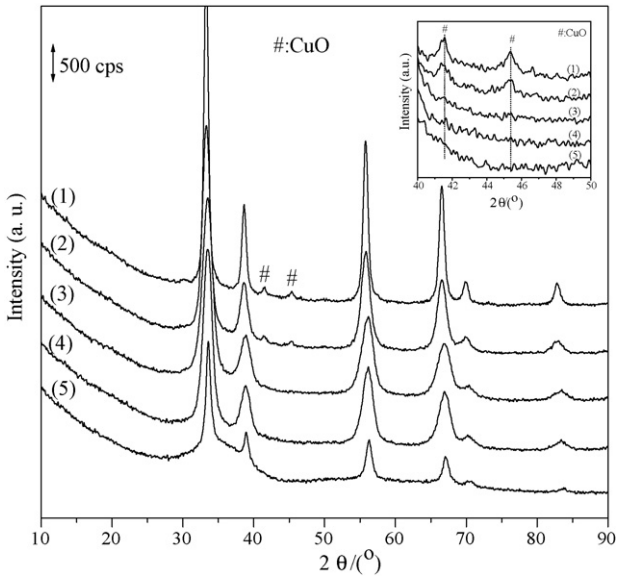


**Fig. 2.** XRD patterns of the samples calcined at 500 °C: (1) $CuO/CeO_2$-P; (2) $CuO/CeO_2$-MP; (3) $CuO/Ce_{0.9}Ti_{0.1}O_2$; (4) $CuO/Ce_{0.7}Ti_{0.3}O_2$; (5) $CuO/Ce_{0.5}Ti_{0.5}O_2$.

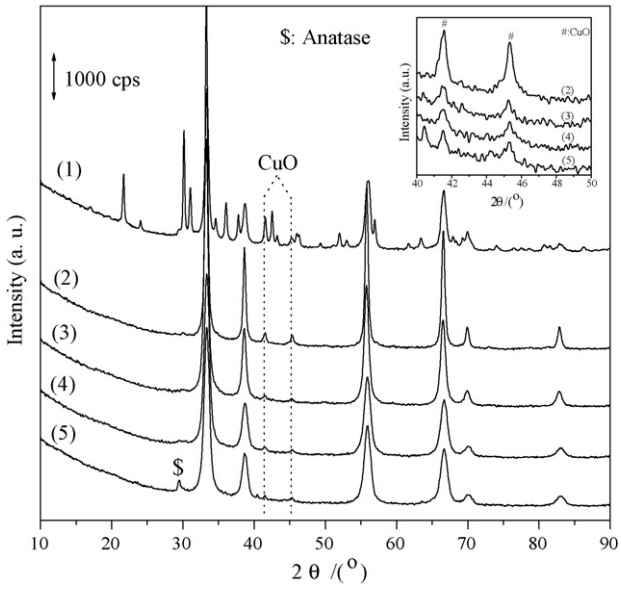


**Fig. 3.** XRD patterns of the aged samples: (1) $CuO/Ce_{0.5}Ti_{0.5}O_2$ (A); (2) $CuO/CeO_2$-P (A); (3) $CuO/CeO_2$-MP (A); (4) $CuO/Ce_{0.9}Ti_{0.1}O_2$ (A); (5) $CuO/Ce_{0.7}Ti_{0.3}O_2$ (A).

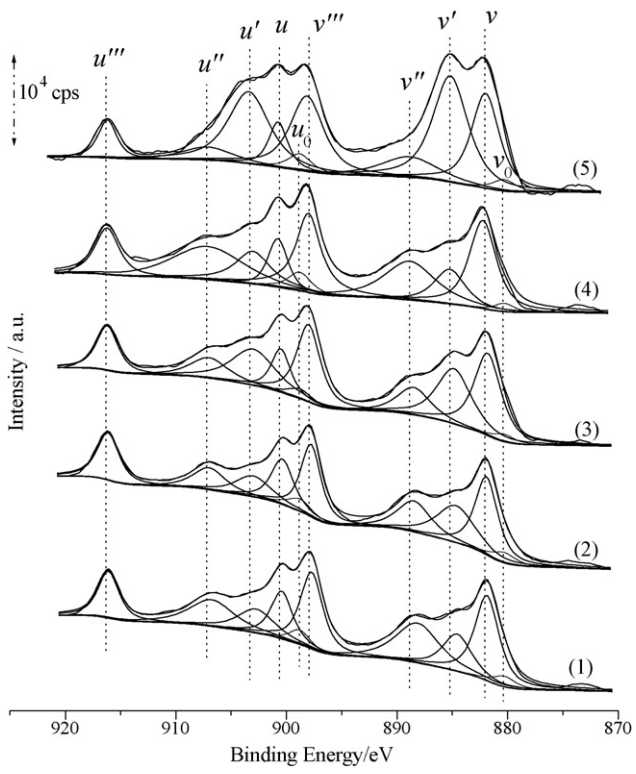


**Fig. 4.** XPS Ce3d spectra of the fresh samples: (1) $CuO/CeO_2$-P; (2) $CuO/CeO_2$-MP; (3) $CuO/Ce_{0.9}Ti_{0.1}O_2$; (4) $CuO/Ce_{0.7}Ti_{0.3}O_2$; (5) $CuO/Ce_{0.5}Ti_{0.5}O_2$.

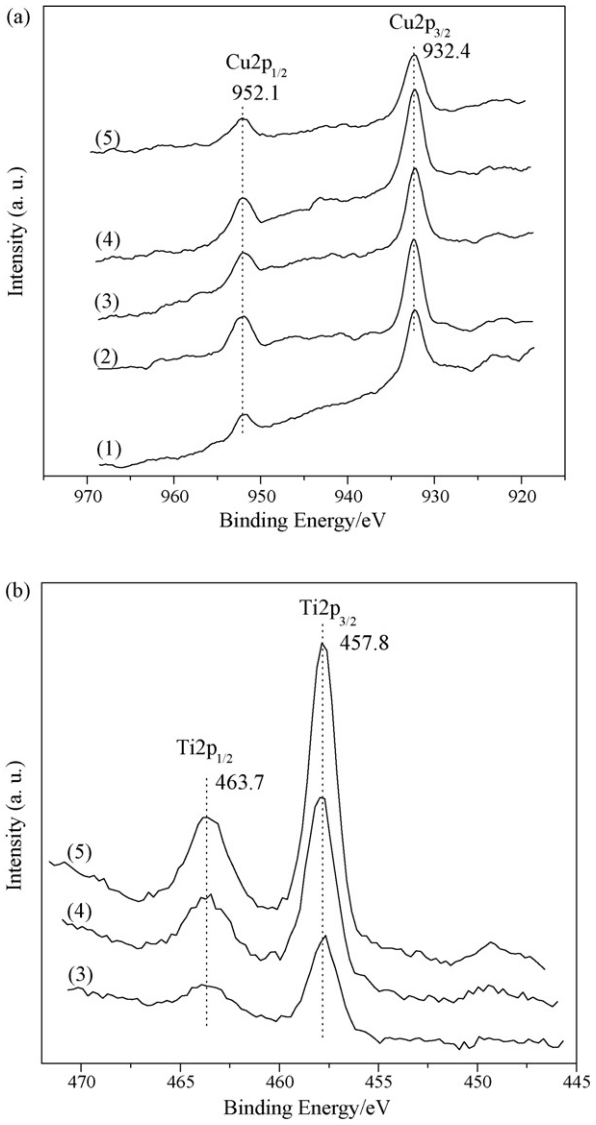


**Fig. 5.** XPS Cu2p (a) and Ti2p spectra (b) of the fresh samples: (1) $CuO/CeO_2$-P; (2) $CuO/CeO_2$-MP; (3) $CuO/Ce_{0.9}Ti_{0.1}O_2$; (4) $CuO/Ce_{0.7}Ti_{0.3}O_2$; (5) $CuO/Ce_{0.5}Ti_{0.5}O_2$.

incorporated into ceria lattice to form solid solution, not only resulting in the shrinkage of crystal lattice due to its smaller radius ($r_{Ti^{4+}} = 0.068$ nm and $r_{Ce^{4+}} = 0.094$ nm) [10] but also inhibiting the crystal growth of the cubic $CeO_2$ phase. After aging treatment, the lattice parameters of $CeO_2$ changed very little, compared with the fresh samples, but the sample $CuO/Ce_{0.5}Ti_{0.5}O_2$ is an exception, whose lattice parameter of $CeO_2$ increased obviously after aging at 700 °C. In the sample $CuO/Ce_{0.5}Ti_{0.5}O_2$, the content of Ti is the highest, which may accelerate the agglomeration of Ti itself at high temperature, inducing the migration of some Ti from the lattice of $CeO_2$, which leads to the more obvious increase of the lattice parameter for $CeO_2$.

XPS analysis was performed in order to gain the binding energies and ratios of surface atoms. In Fig. 4, the experimental and fitted Ce3d spectra of all the fresh samples are presented. The fitting process was referred to literature [19]. The relative content of two cerium species of $Ce^{3+}$ can be determined by $Ce^{3+}/(Ce^{3+} + Ce^{4+})$ where $Ce^{3+} = (u' + u_0 + v' + v_0)$ and $Ce^{4+} = (u''' + u'' + u + v''' + v'' + v)$. The calculated percentages of $Ce^{3+}$ are listed in Table 2. It can be seen that the portions of $Ce^{3+}$ component in the samples with Ce/Ti ratio of 1:9 and 5:5 are relatively high, implying the presence of more oxygen vacancies on the surface of these two samples.

Fig. 5 shows the XPS spectra of Cu2p and Ti2p for the fresh samples. In Fig. 5(a), the peaks centered at 932.4 and 952.1 eV represent the $Cu2p_{3/2}$ and $Cu2p_{1/2}$, respectively. The $Cu2p_{3/2}$ value (932.4 eV) is a little lower than that of CuO, 933.6 eV [20]. At the same time, there is no evident satellite at 940–945 eV. Therefore, it is inferred that some reduced copper species are present on the surface of

**Table 2**
Surface characterization results from XPS test

| Sample | Surface atoms percentage % | | | | Ti/Ce | | $Ce^{3+}/Ce_{tot}$ [a] |
|---|---|---|---|---|---|---|---|
| | $O_L$ [b] | Cu | Ce | Ti | Nominal | Experimental | |
| $CuO/CeO_2$-P | 42.9 | 3.6 | 17.3 | 0 | 0 | 0 | 0.22 |
| $CuO/CeO_2$-MP | 43.6 | 5.1 | 17.3 | 0 | 0 | 0 | 0.27 |
| $CuO/Ce_{0.9}Ti_{0.1}O_2$ | 42.3 | 4.3 | 13.4 | 4.6 | 0.11 | 0.34 | 0.34 |
| $CuO/Ce_{0.7}Ti_{0.3}O_2$ | 42.6 | 4.5 | 10.1 | 10.1 | 0.43 | 1.00 | 0.22 |
| $CuO/Ce_{0.5}Ti_{0.5}O_2$ | 43.0 | 2.5 | 7.0 | 14.4 | 1.00 | 2.06 | 0.46 |

[a] $Ce^{3+}/Ce_{tot} = Ce^{3+}/(Ce^{4+} + Ce^{3+})$.

[b] $O_L$ represents lattice oxygen around 530 eV, calculated by decomposing the O1s spectra and subtracting surface adsorption oxygen.

these samples, though XRD results only show the existence of CuO in these samples. However, it is impossible to distinguish $Cu^0$ and $Cu_2O$ due to their identical values of $Cu2p_{3/2}$ binding energy. The same phenomenon has been frequently found for $CuO/CeO_2$ and $CuO/CeO_2$–$ZrO_2$ systems [8]. It is reported that the binding energy of $Ti2p_{3/2}$ in pure $TiO_2$ is 458.8 eV [21]. In Fig. 5(b), the binding energy of 457.8 eV for $Ti2p_{3/2}$ is observed, suggesting that the main Ti species are $Ti^{4+}$. A little lower binding energy does not mean the existence of $Ti^{3+}$ on the surface of the samples since the Ti2p core level is relatively narrow and symmetric. The difference of binding energy of $Ti2p_{3/2}$ between the catalysts and pure $TiO_2$ may result from the electronic state interaction between Ti and other components in the catalysts.

The percentages of surface atoms of the fresh samples listed in Table 2 show that the content of surface Cu species supported on $CeO_2$-MP is larger than that on $CeO_2$-P. This is related to the larger surface area of the former and the induced higher dispersion of copper species. After Ti doping, the content of surface Cu species in the samples was decreased, since more and more Ti species have occupied the catalyst surface with the amount of Ti increasing. By the comparison of the experimental and nominal Ti/Ce ratios, serious surface enrichment of Ti can be found, especially for the sample with Ti/Ce ratio of 1:9.

### 3.3. Redox properties

In order to study the reducibility of CuO supported on different supports, $H_2$-TPR test was performed for both the fresh and the aged samples, the results of which are shown in Fig. 6. A two-step reduction profile is observed for all the samples in the region below 400 °C, indicating the existence of at least two copper species. In fact, many studies [6,8,22] have investigated the reduction behavior of CuO supported on $CeO_2$ and the two-step reduction process has also been found. It is believed that the peak at lower temperature represents the reduction of highly dispersed CuO strongly interacting with the support while the peak at higher temperature corresponds to the reduction of relatively larger CuO crystallites weakly associated with the support. Therefore, in Fig. 6, the peak at the lowest temperature denoted as α can be attributed to the reduction of highly dispersed copper species strongly interacting with $CeO_2$ or $Ce_{1-x}Ti_xO_2$ mixed supports, while the peak at higher temperature denoted as β may arise from the reduction of larger CuO crystallites weakly interacting with supports. However, these relatively larger CuO crystallites are still XRD-invisible since only the samples without Ti show very weak diffraction peaks assigned to CuO. In addition, it is found that peak α for the fresh sample with Ti/Ce ratio of 5:5 is either very small or completely covered by peak β. Meanwhile, it is surprising that a very large peak appears at higher temperature than that of peak β, which is denoted as δ. The reason will be discussed later.

After aging, peak α of all samples shifted a little to higher temperatures while peak β shifted a lot and it is newly denoted as γ. Since strong diffraction peaks corresponding to CuO can be found in all the aged samples, it is more reasonable to attribute peak γ to the reduction of the larger bulk CuO crystallites. In addition to the reduction peaks of copper species, too much weaker peaks around 450 and 850 °C can be found for some samples in Fig. 6, which should correspond to the reduction of surface and bulk $CeO_2$, as reported in literature [23].

In order to discern the effect of Ti content on the reducibility of the samples, quantitative analysis of $H_2$-TPR profiles was performed and the results are shown in Table 3. The evaluation of the amount of reducible species was made by integrating the areas of the reduction peaks and they are compared with the area of the reduction peaks of pure CuO. From Table 3, it can be seen that the

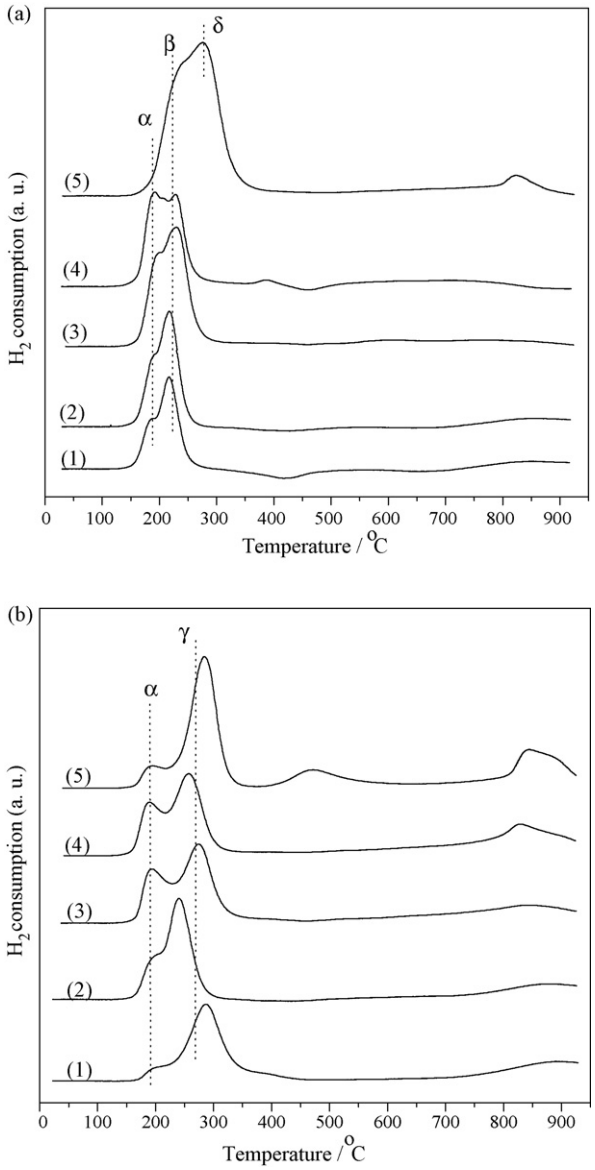


**Fig. 6.** $H_2$-TPR patterns of the fresh (a) and aged samples (b): (1) $CuO/CeO_2$-P; (2) $CuO/CeO_2$-MP; (3) $CuO/Ce_{0.9}Ti_{0.1}O_2$; (4) $CuO/Ce_{0.7}Ti_{0.3}O_2$; (5) $CuO/Ce_{0.5}Ti_{0.5}O_2$.

temperature of peak α in all the fresh samples are almost identical except for the sample $CuO/Ce_{0.5}Ti_{0.5}O_2$ while the corresponding $H_2$ consumptions are various. The sample with the support prepared by modified method shows larger $H_2$ consumption than that with the support prepared by conventional precipitation, implying that more highly dispersed surface copper species strongly interacting with $CeO_2$ are present on the former. Doping Ti in $CeO_2$ support with Ti/Ce ratio of 1:9 and 3:7 further increases the amount of such copper species to a large extent. However, when the ratio was increased to 5:5, peak α became very small and it was difficult to split it from peak β. The reason is surmised from the XPS results above. The surface Cu content in this sample is the lowest and much more Ti species have occupied catalyst surface, which may cover the finely dispersed copper species, therefore, nearly no peak α is detected for this sample. After aging, the agglomeration of Ti may leave some copper sites exposed, giving a small reduction peak in its TPR profile.

According to the content of Cu (6 wt%), the calculated stoichiometric amount of $H_2$ required for the complete reduction of all the

**Table 3**
$H_2$ consumption amount of the fresh and aged samples

| Sample | Peak α | | Peak β | | Peak γ/δ | | Total amount ($\mu$mol g$^{-1}$) |
|---|---|---|---|---|---|---|---|
| | $T$ (°C) | Amount ($\mu$mol g$^{-1}$) | $T$ (°C) | Amount ($\mu$mol g$^{-1}$) | $T$ (°C) | Amount ($\mu$mol g$^{-1}$) | |
| $CuO/CeO_2$-P | 188 | 212 | 217 | 686 | – | – | 898 |
| $CuO/CeO_2$-MP | 188 | 285 | 217 | 831 | – | – | 1116 |
| $CuO/Ce_{0.9}Ti_{0.1}O_2$ | 190 | 565 | 230 | 1080 | – | – | 1645 |
| $CuO/Ce_{0.7}Ti_{0.3}O_2$ | 190 | 491 | 227 | 824 | – | – | 1315 |
| $CuO/Ce_{0.5}Ti_{0.5}O_2$ | – | – | 236 | 758 | 275 | 2133 | 2891 |
| $CuO/CeO_2$-P (A) | 205 | 95 | – | – | 288 | 851 | 946 |
| $CuO/CeO_2$-MP (A) | 202 | 215 | – | – | 240 | 768 | 983 |
| $CuO/Ce_{0.9}Ti_{0.1}O_2$ (A) | 195 | 396 | – | – | 271 | 802 | 1198 |
| $CuO/Ce_{0.7}Ti_{0.3}O_2$ (A) | 191 | 343 | – | – | 256 | 790 | 1133 |
| $CuO/Ce_{0.5}Ti_{0.5}O_2$ (A) | 202 | 138 | – | – | 284 | 1167 | 1305 |

Cu species from CuO to $Cu^0$ is 938 $\mu$mol g$^{-1}$. However, the total $H_2$ consumptions below 400 °C for all the samples have noticeably exceeded 938 $\mu$mol g$^{-1}$ except for $CuO/CeO_2$-P. It is indicated in literature [24,25] that the reduction of support $CeO_2$ can be greatly enhanced by the reduced copper species via hydrogen spillover as noble metals promote the reduction of supports oxides [26]. From Table 3, it can be seen that the enhancement effect is more obvious for the sample $CuO/Ce_{0.5}Ti_{0.5}O_2$ with the largest Ti content, suggesting that Ti doping can increase the reduction degree of $CeO_2$ support. Therefore, peak δ in Fig. 6(a) mainly originates from the reduction of $CeO_2$ associated with Cu species. However, it is surprising that the total $H_2$ consumption (2891 $\mu$mol g$^{-1}$) below 400 °C has exceeded the theoretical $H_2$ consumption required for the complete reduction of both $Cu^{2+}$ to $Cu^0$ and $Ce^{4+}$ to $Ce^{3+}$ in the sample $CuO/Ce_{0.5}Ti_{0.5}O_2$ (2773 $\mu$mol g$^{-1}$). So it is inferred that the reduction of Ti species may be also enhanced though it is hard to reduce pure $TiO_2$ below 400 °C. In order to make this assumption clear, the $H_2$-TPR test for pure $TiO_2$ with a specific surface area of 10 m$^2$/g, pure CuO derived from decomposition of copper nitrate, and CuO supported on $TiO_2$ (7.5 wt%) were performed, the results are shown in Fig. 7. It is observed that the reduction of pure $TiO_2$ is almost neglectable as expected. The calculated area of reduction peak below 500 °C for 30 mg $CuO/TiO_2$ (7.5 wt%) is about 1.6 times as large as that for 2.25 mg pure CuO. If no Ti species were reduced in the sample $CuO/TiO_2$, the two areas should be equal or close to each other because of the same content of CuO in these two samples. Therefore, the reduction degree of Ti species should be enhanced by Cu species in the sample $CuO/TiO_2$. In Fig. 7, the sharp peak at 288 °C may be ascribed to the reduction of bulk CuO and the shoulder peak at 228 °C can be assigned to the reduction of surface dispersed Cu species while the other shoulder peak at a higher temperature of 358 °C may result from the reduction of Ti species from $Ti^{4+}$ to $Ti^{3+}$. Therefore, it is convinced that the reduction of Ti species should be included in peak δ in Fig. 6(a) for the sample $CuO/Ce_{0.5}Ti_{0.5}O_2$ with the largest Ti content.

In summary, the $H_2$-TPR results show that more highly dispersed copper species strongly interacting with $CeO_2$ can be formed on the $CeO_2$ prepared by surfactant-modified method and Ti doping in the support with Ti/Ce ratio of 1:9 and 3:7 can further increase the amount of such copper species. However, when Ti/Ce ratio reaches to 5:5, such copper species is greatly decreased while the reduction of the support $Ce_{1-x}Ti_xO_2$ is remarkably enhanced.

### 3.4. Catalytic performance and structure–activity relationship

The light-off curves of the fresh and aged samples are presented in Figs. 8 and 9, respectively. It can be seen that the activity for CO oxidation increases with the elevation of the reaction temperature for both the fresh and the aged samples. After aging, the activities of all the samples are decreased due to the sintering of the samples. For the fresh samples, the difference between $Cu/CeO_2$-MP and $Cu/CeO_2$-P is neglectable. However, when they are aged at high

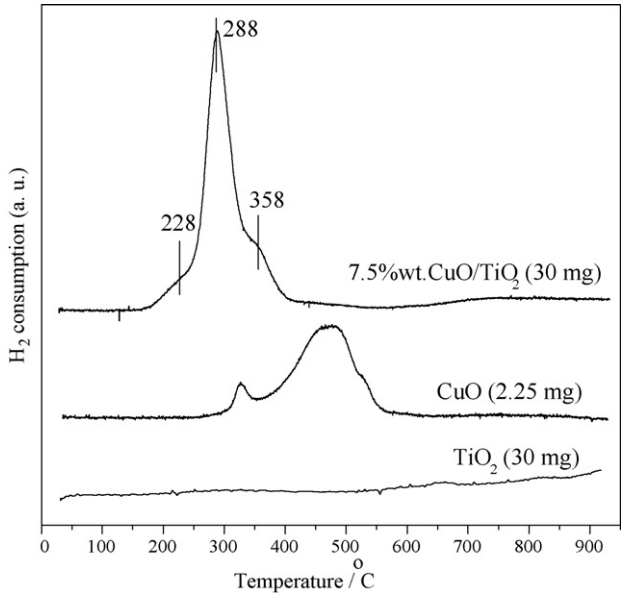


**Fig. 7.** The comparison of $H_2$-TPR patterns of pure CuO, $TiO_2$ and $CuO/TiO_2$ samples.

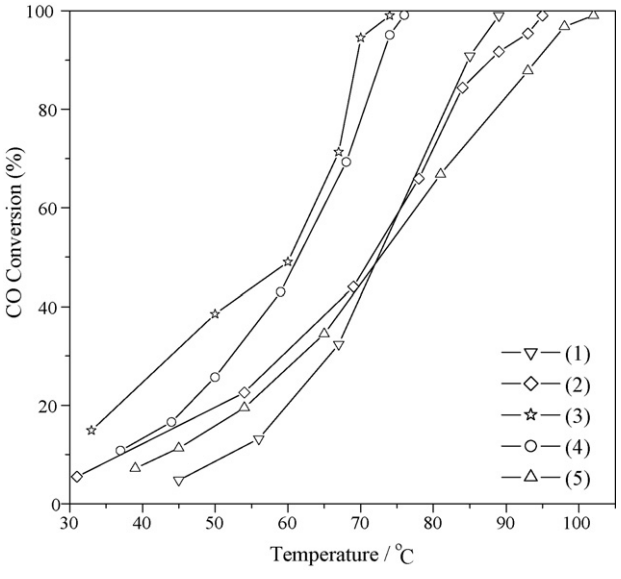


**Fig. 8.** The activities of the fresh samples: (1) $CuO/CeO_2$-P; (2) $CuO/CeO_2$-MP; (3) $CuO/Ce_{0.9}Ti_{0.1}O_2$; (4) $CuO/Ce_{0.7}Ti_{0.3}O_2$; (5) $CuO/Ce_{0.5}Ti_{0.5}O_2$.

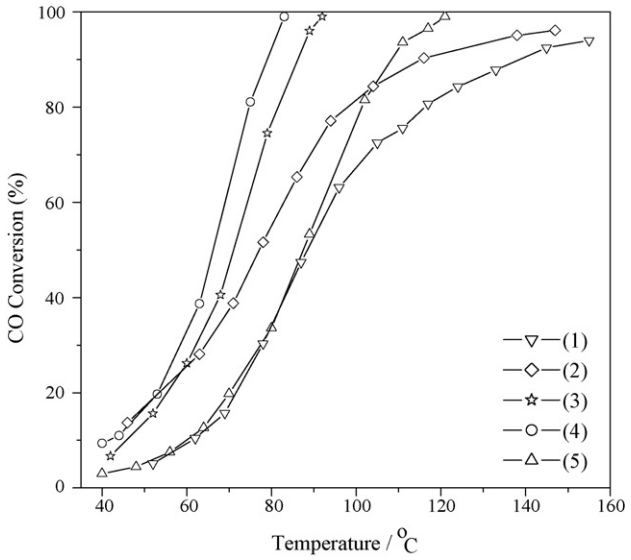


**Fig. 9.** The activities of the aged samples: (1) $CuO/CeO_2$-P (A); (2) $CuO/CeO_2$-MP (A); (3) $CuO/Ce_{0.9}Ti_{0.1}O_2$ (A); (4) $CuO/Ce_{0.7}Ti_{0.3}O_2$ (A); (5) $CuO/Ce_{0.5}Ti_{0.5}O_2$ (A).

temperature, the difference is enlarged, especially at high temperature region. This may be due to the fact that the surface area of the aged sample $Cu/CeO_2$-P (A) is only 7 $m^2/g$, and the $H_2$-TPR results also show that the amount of the highly dispersed copper species strongly interacting with $CeO_2$ is much smaller in $CuO/CeO_2$-P (A) than in $CuO/CeO_2$-MP (A). Such highly dispersed copper species should be related to the activities of the sample, as suggested by Luo et al. [4] that well-dispersed CuO was responsible for the high catalytic activity for low-temperature CO oxidation while the bulk CuO crystallites contributed little to the activity. From the view of pore volume and specific surface area in Table 1, it is obvious that the sample with the support $CeO_2$ prepared by surfactant-modified method possesses higher thermal stability.

As observed from Figs. 8 and 9, Ti doping in $CeO_2$ support with Ti/Ce ratios of 1/9 and 3/7 has greatly improved the activities of both the fresh and the aged samples. The light-off temperatures at which the conversion of CO achieves 50% are always below 70 °C. The combined results of BET and XRD show that when Ti is doped in the ratios of 1/9 and 3/7, the surface areas are increased and the crystallite sizes of $CeO_2$ are decreased a lot, which is favorable to the dispersion of copper species on the supports and the contact between copper and cerium species. Consequently, much more highly dispersed copper species can be reduced at low temperatures as reflected in their $H_2$-TPR profiles. However, when the ratio of Ti/Ce is increased to 5:5, the activity is decreased. The XPS results have shown that in this sample the surface copper content is the lowest and the surface concentration of Ti is very high, and the $H_2$-TPR results have also indicated that the least dispersed copper species corresponding to peak α in Fig. 6 are present in this sample, all these factors are responsible for the decrease in activity. In a summary, Ti doping in $CeO_2$ with a proper ratio is crucial to the improvement of the catalytic activity of $Cu/CeO_2$ catalyst for low-temperature CO oxidation.

In order to investigate the stability of the proposed catalysts, the catalyst $CuO/Ce_{0.9}Ti_{0.1}O_2$ calcined at 500 °C was selected to perform stability test. The reactants and space velocity are the same with those used in the activity test above but the reaction temperature was fixed at 75 °C, at which 100% CO conversion was achieved. After a continuous test of 12 h, the CO conversion over $CuO/Ce_{0.9}Ti_{0.1}O_2$ is still 99%, suggesting the very high stability of this catalyst.

## 4. Conclusions

(1) The support $CeO_2$-MP prepared by surfactant-modified method with P123 involved in the precipitation process shows larger specific surface areas and smaller crystallite size compared to the one prepared by conventional precipitation method. The supported catalyst using $CeO_2$-MP as support shows much higher thermal stability and catalytic activity for low-temperature CO oxidation, due to the presence of more highly dispersed Cu species strongly interacting with $CeO_2$.

(2) Ti doping in the support $CeO_2$ can further increase its surface area and decrease the crystallite size of $CeO_2$ due to the formation of Ti–Ce oxide solid solution. However, the atomic ratio of Ti/Ce is sensitive to the dispersion of Cu species and its reducibility. The proper ratio of Ti/Ce should be 1:9 or 3:7, which ensures the presence of more highly dispersed copper species strongly interacting with $CeO_2$, and therefore enhances the oxidation activity of the catalysts. However, further increase of Ti/Ce ratio to 5:5 leads to high surface concentration of Ti, decreasing the surface finely dispersed copper species and weakening the interaction between Cu and Ce species, which are unfavorable to catalytic activity.

## Acknowledgements

This work is financially supported by the "863 Program" of the Ministry of Science & Technology of China (No. 2006AA06Z348) and the National Natural Science Foundation of China (No. 20676097). The authors are also grateful to the support from the Program of New Century Excellent Talents in Universities of China (NCET-07-0599), the Cheung Kong Scholar Program for Innovative Teams of the Ministry of Education (No. IRT0641) and the Program for Introducing Talents of Discipline to Universities of China (No. B06006).

## References

[1] M. Skoglundh, E. Fridell, Strategies for enhancing low-temperature activity, Top. Catal. 28 (2004) 79–87.
[2] G. Avgouropoulos, T. Ioannides, H.K. Matralis, J. Batista, S. Hocevar, CuO-$CeO_2$ mixed oxide catalysts for the selective oxidation of carbon monoxide in excess hydrogen, Catal. Lett. 73 (2001) 33–40.
[3] X.C. Zheng, S.H. Wu, S.P. Wang, S.R. Wang, S.M. Zhang, W.P. Huang, The preparation and catalytic behavior of copper-cerium oxide catalysts for low-temperature carbon monoxide oxidation, Appl. Catal. A 283 (2005) 217–223.
[4] M.F. Luo, J.M. Ma, J.Q. Lu, Y.P. Song, Y.J. Wang, High-surface area CuO-$CeO_2$ catalysts prepared by a surfactant-templated method for low-temperature CO oxidation, J. Catal. 246 (2007) 52–59.
[5] G.W. Graham, H.W. Jen, R.W. McCabe, A.M. Straccia, L.P. Haack, Characterization of model automotive exhaust catalysts: Pd on Zr-rich ceria-zirconia supports, Catal. Lett. 67 (2001) 99–105.
[6] M.F. Luo, Y.J. Zhong, X.X. Yuan, X.M. Zheng, TPR and TPD studies of $CuO/CeO_2$ catalysts for low temperature CO oxidation, Appl. Catal. A 162 (1997) 121–131.
[7] S.P. Wang, X.C. Zheng, X.Y. Wang, S.R. Wang, S.M. Zhang, L.H. Yu, W.P. Huang, S.H. Wu, Comparison of $CuO/Ce_{0.8}Zr_{0.2}O_2$ and $CuO/CeO_2$ catalysts for low-temperature CO oxidation, Catal. Lett. 105 (2005) 163–168.
[8] S.M. Zhang, W.P. Huang, X.H. Qiu, B.Q. Li, X.C. Zheng, S.H. Wu, Comparative study on catalytic properties for low temperature CO oxidation of $Cu/CeO_2$ and $CuO/CeO_2$ prepared via solvated metal atom impregnation and conventional impregnation, Catal. Lett. 80 (2002) 41–46.
[9] T.Y. Zhang, S.P. Wang, Y. Yu, Y. Su, X.Z. Guo, S.R. Wang, S.M. Zhang, S.H. Wu, Synthesis, characterization of $CuO/Ce_{0.8}Sn_{0.2}O_2$ catalysts for low-temperature CO oxidation, Catal. Commun. 9 (2008) 1259–1264.
[10] M.F. Luo, J. Chen, L.S. Chen, J.Q. Lu, Z.C. Feng, C. Li, Structure and redox properties of $Ce_xTi_{1-x}O_2$ solid solution, Chem. Mater. 13 (2001) 197–202.
[11] H.Q. Zhu, Z.F. Qin, W.J. Shan, W.J. Shen, J.G. Wang, $Pd/CeO_2$–$TiO_2$ catalyst for CO oxidation at low temperature: a TPR study with $H_2$ and CO as reducing agents, J. Catal. 225 (2004) 267–277.
[12] Z.Q. Zou, M. Meng, Y.Q. Zha, The effect of dopant Cu, Fe, Ni or La on the structures and properties of mesoporous Co-Ce-O compound catalysts, J. Alloys Compd. 470 (2009) 96–106.
[13] Z.Q. Zou, M. Meng, Y.Q. Zha, Y. Liu, Dual templates assisted preparation and characterization of highly thermostable multicomponent mesoporous material La-Ce-Co-Zr-O used for low-temperature CO oxidation, J. Mater. Sci. 43 (2008) 1958–1965.

[14] Z.Q. Zou, M. Meng, Q. Li, Y.Q. Zha, Surfactants-assisted synthesis and characterizations of multicomponent mesoporous materials Co-Ce-Zr-O and Pd/Co-Ce-Zr-O used for low-temperature CO oxidation, Mater. Chem. Phys. 109 (2008) 373–380.
[15] D.A.M. Monti, A. Baiker, Temperature-programmed reduction, parametric sensitivity and estimation of kinetic parameters, J. Catal. 83 (1983) 323–335.
[16] K.S.W. Sing, D.H. Everett, R.A. Haul, L. Moscow, R.A. Pierotti, J. Rouquerol, T. Siemieniewska, Reporting physisorption data for gas/solid systems with special reference to the determination of surface area and porosity, Pure Appl. Chem. 57 (1985) 603–619.
[17] J.L. Cao, Y. Wang, T.Y. Zhang, S.H. Wu, Z.Y. Yuan, Preparation, characterization and catalytic behavior of nanostructured mesoporous $CuO/Ce_{0.8}Zr_{0.2}O_2$ catalysts for low-temperature CO oxidation, Appl. Catal. B 78 (2008) 120–128.
[18] J. Rynkowski, J. Farbotko, R. Touroude, L. Hilaire, Redox behaviour of ceria-titania mixed oxides, Appl. Catal. A 203 (2000) 335–348.
[19] M.A. Henderson, C.L. Perkins, M.H. Engelhard, S. Thevuthasan, C.H.F. Peden, Redox properties of water on the oxidized and reduced surfaces of $CeO_2$ (1 1 1), Surf. Sci. 526 (2003) 1–18.
[20] G. Avgouropoulos, T. Ioannides, Selective CO oxidation over $CuO\text{-}CeO_2$ catalysts prepared via the urea–nitrate combustion method, Appl. Catal. A 244 (2003) 155–167.
[21] J. Fang, X.Z. Bi, D.J. Si, Z.Q. Jiang, W.X. Huang, Spectroscopic studies of interfacial structures of $CeO_2$–$TiO_2$ mixed oxides, Appl. Surf. Sci. 253 (2007) 8952–8961.
[22] G. Avgouropoulos, T. Ioannides, Effect of synthesis parameters on catalytic properties of $CuO\text{-}CeO_2$, Appl. Catal. B 67 (2006) 1–11.
[23] C. de Leitenburg, A. Trovarelli, J. Kašpary, A temperature-programmed and transient kinetic study of $CO_2$ activation and methanation over $CeO_2$ supported noble metals, J. Catal. 166 (1997) 98–107.
[24] F. Marinño, B. Schönbrod, M. Moreno, M. Jobbágy, G. Baronetti, M. Laborde, CO preferential oxidation over CuO–$CeO_2$ catalysts synthesized by the urea thermal decomposition method, Catal. Today 133–135 (2008) 735–742.
[25] A. Gómez-Cortés, Y. Márquez, J. Arenas-Alatorre, G. Díaz, Selective CO oxidation in excess of $H_2$ over high-surface area $CuO/CeO_2$ catalysts, Catal. Today 133–135 (2008) 743–749.
[26] P. Fornasiero, J. Kašpary, V. Sergo, M. Graziani, Redox behavior of high-surface-area Rh-, Pt-, and Pd-loaded $Ce_{0.5}Zr_{0.5}O_2$ mixed oxide, J. Catal. 182 (1999) 56–69.